Research Article | Vol. 27, No. 8 | 15 Apr 2019 | OPTICS EXPRESS 11361
Optics EXPRESS

Metallic carbon nanotube-based saturable absorbers for holmium-doped fiber lasers

MARIA PAWLISZEWSKA,[1,*] ANNA DUŻYŃSKA,[2] MARIUSZ ZDROJEK,[2] AND JAROSŁAW SOTOR[1,3]

[1]*Laser & Fiber Electronics Group, Faculty of Electronics, Wrocław University of Science and Technology, Wybrzeże Wyspiańskiego 27, 50-370, Wrocław, Poland*
[2]*Faculty of Physics, Warsaw University of Technology, Koszykowa 75, 00-662 Warsaw, Poland*
[3]*jaroslaw.sotor@pwr.edu.pl*
[*]*maria.pawliszewska@pwr.edu.pl*

Abstract: In 2003, carbon nanotubes opened a new field of research on nanomaterial-based mode-locked fiber lasers. They maintain popularity in the ultrafast laser community due to their broadband operation, relatively high damage threshold, and tunable optical properties. Here we show that metallic carbon nanotube-based thin film fabricated by vacuum filtration technique can be used as a saturable absorber in holmium-doped fiber laser operating in anomalous and normal dispersion regimes. Scaling the absorbers modulation depth by adjusting the film thickness was observed. The Fourier transform limited 6.65 nm wide optical solitons in anomalous dispersion regime were generated. Utilizing stretched-pulse regime greatly improves the laser performance - 212 fs pulses reach the energy of 3.79 nJ.

1. Introduction

The first demonstration of an ultrafast fiber laser mode-locked with carbon nanotube saturable absorber (CNT-SA) which took place in 2003 [1] opened a new area of research on nanomaterial-based saturable absorbers. Since that time significant effort was invested to explore many forms of mode-locked lasers utilizing CNT-SAs [2–18]. Among them, ytterbium [6], bismuth [7], praseodymium [8], erbium [9], thulium [10], and holmium-doped [11] fiber lasers can be found. Devices capable of wavelength tuning [12–14] and operation in uncommon dispersion regimes, such as stretched-pulse [15, 16] or all-normal dispersion [17] were presented. The latter applications demand a relatively high modulation depth of the saturable absorber, which can be scaled by manipulating the material thickness in a CNT-SA [18], or by utilizing material anisotropy [19]. The comprehensive portfolio of CNT-SA-based lasers manifests the versatility and wide operation bandwidth of the nanomaterial. Its other significant advantages include relatively high damage threshold [20], possibility to use in transmission and reflection modes [21], fast (< 1 ps) relaxation time [22], and simple fabrication which does not require clean room environment [23]. Methods of producing free-standing (polymer-free) films were also presented [24].

Ultrafast holmium-doped fiber lasers, first presented in 2012 [25], are a relatively young family of rare-earth doped fiber lasers. Specific applications of their emission band including surgical procedures [26], light detection and ranging (LIDAR) systems [27], or pumping optical parametric oscillators [28] motivate further exploration of this field. In the last years, several demonstrations of pulsed sources utilizing both artificial [29–31] and real saturable absorbers were presented. So far graphene [32], black phosphorus [33], SESAMs [34] and carbon nanotubes [11] were experimentally confirmed to be capable of operation in the holmium emission band (~2080 nm). Additionally, in our recent research, we have shown that reaching operation in the stretched-pulse dispersion regime is possible [35].

Despite the popularity of CNT-SAs their applicability to holmium-doped fiber lasers was not

#357338 https://doi.org/10.1364/OE.27.011361
Journal © 2019 Received 11 Jan 2019; revised 26 Mar 2019; accepted 27 Mar 2019; published 9 Apr 2019

Optics EXPRESS

extensively researched in terms of stability, scalability, and operation in different dispersion regimes. Moreover, CNT-SAs demonstrated so far consisted of either a mixture of metallic and semiconducting, or exclusively semiconducting CNTs. In such SAs operating in near-infrared spectral range the absorption mechanism is directly related to the energy band gaps (commonly labeled as E_{11}, E_{22} or S_{11}, S_{22}) of semiconducting nanotubes [36, 37]. The metallic CNTs were responsible for the optical absorption mainly in the visible spectral range (higher energy band typically labeled as M_{11}) [37]. According to the Kataura plot [38] these band gaps and therefore the operating optical spectral range is directly dependent on the nanotube diameter. In the case of thin films composed of many individual bundled nanotubes, the band structure is much more complicated. Their interactions even lead to opening the band gap in metallic CNTs [39, 40] which enables optical absorption in the near-infrared spectral range. Furthermore, the optical absorption process in metallic CNTs at energies lower than those related to van Hove singularity M_{11} is possible also due to excitations effects [41] and hot Dirac fermions [42].

To the best of our knowledge, we present for the first time that metallic single-walled CNTs can serve as a SA in the 2 µm spectral range. The polymer-free metallic CNT films with varying thicknesses are characterized by SEM, absorbance measurements, and Raman spectra. Their uniformity is confirmed through optical transmittance measurements. Fully fiberized CNT-SAs are formed by depositing the films on a fiber connector end facet, and their nonlinear optical parameters are measured. We experimentally determine the influence of CNT film thickness on the performance of a holmium-doped fiber laser operating in anomalous dispersion regime. Optical pulses with duration in the 680-990 fs range are obtained. CNT-SA-based mode-locking stability is confirmed by 70-hour operation test. Further, to show the versatility of the fabricated CNT-SAs, a stretched-pulse all-fiber cavity was effectively designed. After performing output power scaling, the generation of significantly shorter (212 fs) and higher-energy (3.79 nJ) pulses was achieved.

2. Carbon nanotube film fabrication and characterisation

The metallic single-walled carbon nanotube (m-SWCNT) films were fabricated using the following formula. 1 mg of pure dry m-SWCNTs from NanoIntegris (purity 99%, mean length ~0.5 µm, mean diameter 1.4 nm) was dispersed in water with 1% weight per volume (w/v) sodium dodecyl sulfate (≥99% Carl Roth) using bath sonication for 5h (in cool water to prevent heating). To separate the homogeneous suspension from bundles of nanotubes, the dispersion was twice centrifuged at 8000 rpm for 10 min. Next, the supernatant was decanted and diluted in two parts of deionized water. The prepared suspension was used to produce the m-SWCNT thin films by a vacuum filtration method [23]. In short, an appropriate amount of carbon nanotubes suspension was filtered onto the mixed cellulose ester membrane (MCE, 0.025 µm pore-size, 25 diameter, from Millipore) to achieve a specified thickness of the m-SWCNT films. After film forming, the residual surfactant was subsequently washed away with a large amount of deionized water. A dry filtration membrane with the attached nanotube film was cut to approximately 5 x 5 mm^2 pieces and immersed directly into an acetone bath to quick dissolution of MCE membrane. The acetone was refreshed several times to ensure effectively complete removal of MCE. Then acetone was replaced by the isopropanol/water solution with the ratio of 1:1 and each m-SWCNT film was picked up on a fiber connector or flat substrate (SiO_2/Si or glass) and allowed to dry. The thickness of all fabricated films was measured with AFM Veeco Icon system.

As a first step, initial structural and optical characterization of the m-SWCNT films properties was performed. For simplicity, films were transferred on flat substrates . Figure 1(a) shows a typical scanning electron microscope (SEM) image of the carbon nanotube network (here for 50 nm film thickness obtained with Raith eLine PLUS microscope). Clearly, our vacuum filtered film is continuous, homogenous and pure, without residual contaminations. Nanotubes in the whole film are randomly and tightly arranged, which is typical of all films thicknesses

Optics EXPRESS

used in this work (SEM images for thicker films look very similar [43]). The m-SWCNT films were transferred on the Si/SiO_2 substrate and on a soda-lime glass for Raman and absorbance measurements, respectively. The absorbance spectrum for a 100 nm and 200 nm thick m-SWCNT film in the 300-3000 nm range obtained with a Cary 5000 UV-Vis-NIR spectrometer is presented in Fig. 1(b). For the wavelength from 500 to 800 nm a characteristic M_{11} band is observed, which confirms that nanotubes used for film preparation are only metallic. Raman spectrum in Fig. 1(c) shows typical carbon nanotube modes G and G', including the RBM band, which appears only for single-walled carbon nanotubes. Presence of a relatively low D peak confirms that analyzed films are pure and contain rather few defects (probably connected to nanotube close packing inside film). The Raman spectra were detected using the inVia Qontor Renishaw spectrometer with a 532 nm (2.33 eV) laser excitation line in a backscattering configuration.

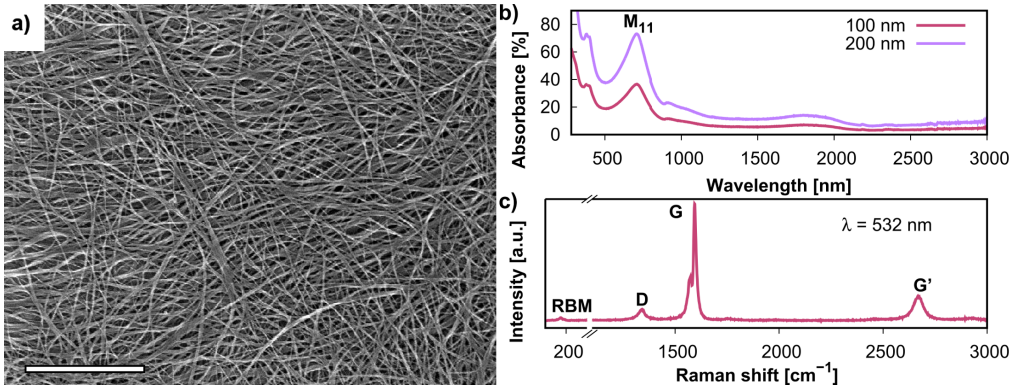

Fig. 1. SEM image of the m-SWCNT film with thickness 50 nm; scale bar represents 800 nm (a). VIS-IR absorbance spectrum of a 100 nm and 200 nm thick m-SWCNT film (b). Raman spectrum of the film shown on SEM image (c).

To investigate the uniformity of the fabricated samples, their optical transmittance was measured in 25 positions of the sample in a 5 x 5 mm^2 area. The chosen measurement wavelength was 2080 nm, which corresponds to the Ho-fiber emission maximum. For 100 nm and 200 nm thick samples (Figs. 2(a) and 2(b), respectively), the differences in transmission did not exceed 1%. The measurements were conducted with a Fourier-transform spectrometer (Thermo Scientific Nicolet iS50).

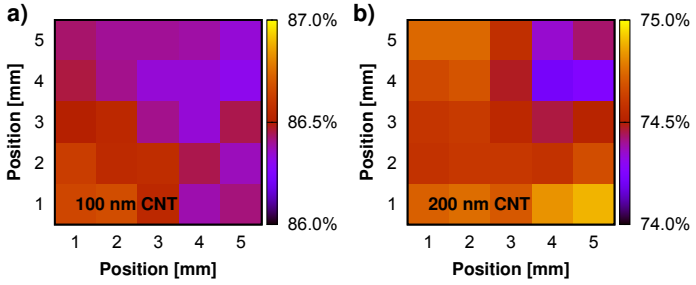

Fig. 2. Spatial linear transmission measured across the 100 nm (a) and 200 nm (b) thick m-SWCNT samples (measured with a 1 mm spatial step at the wavelength of 2080 nm).

The CNT-SAs were fabricated by placing the m-SWCNT film on a fiber connector end facet and joining it with a clean fiber connector. CNT-SAs with film thicknesses of 100, 200, 300 and 400 nm were measured in a fiberized equivalent of a Z-scan setup [44]. The samples were

Optics EXPRESS

illuminated with 1.2 ps pulses centered at 1950 nm with varying average power - therefore their nonlinear transmittance could be recorded. The acquired data were fitted with a fast saturable absorber model [45], and the fitted modulation depths and non-saturable losses are indicated on corresponding graphs shown in Fig. 3. The measured sample transmission for low-intensity excitation is in good agreement with the values acquired during linear transmission measurement.

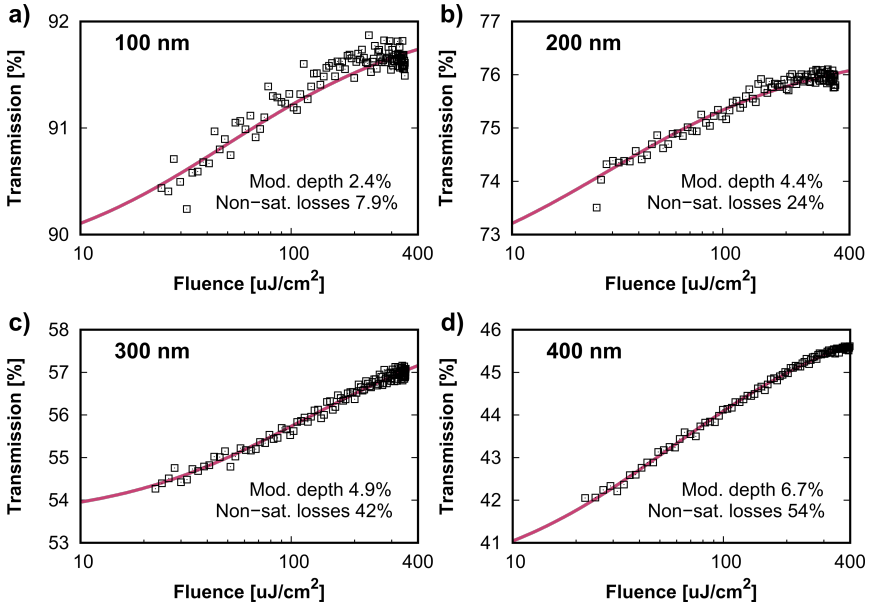

Fig. 3. Power-dependent transmittance of a 100 nm (a), 200 nm (b), 300 nm (c) and 400 nm (d) CNT-SA. Squares - experimental data, red curve - theoretical fit.

3. Mode-locked soliton laser

The schematic of an all-fiber ring laser cavity is presented in Fig. 4(a). A thulium-doped fiber laser is used as a pumping source. The 1950/2080 nm wavelength division multiplexer (WDM) introduces the pump to the laser cavity. As a gain medium, 180 cm of commercially available holmium-doped fiber (HDF, Nufern SM-HDF-10/130) is used. In the later parts of the experiment, an additional dispersion compensating fiber (DCF, Nufern UHNA4) is added to the cavity in order to reach stretched-pulse and net-normal dispersion regimes. Various coupling ratios of the output coupler (between 10%-70%) were utilized to analyze its influence on the laser operation. As a saturable absorber, CNT-SAs described in previous sections with 100 and 200 nm thicknesses were used. In order to increase the optical absorption, two fiber connectors with deposited m-SWCNT films were connected to each other.

Figures 4(b)-4(d) show the performance of a solitonic laser with a 400 nm thick CNT-SA and output coupling ratio of 30%. The achieved optical bandwidth of 6.6 nm (Fig. 4(b)) is comparable to our previous experiments where graphene-based SA was used [32]. Repetition frequency of 54.98 MHz corresponding to the cavity length of 3.71 m is presented in Fig. 4(c) along with the radio frequency spectrum measured in a 0-3 GHz span. The measured autocorrelation trace of solitons with 683 fs pulse duration is presented in Fig. 4(d) with a theoretical sech^2 fitting.

The performance of the solitonic laser utilizing saturable absorbers of various thicknesses is presented in Table 1. The best performance in terms of average output power, pulse energy, pulse duration, and optical bandwidth is reached for a 400 nm thick CNT-SA. On the other hand, non-saturable losses that increase with film thickness cause the central wavelength blue shift.

Optics EXPRESS

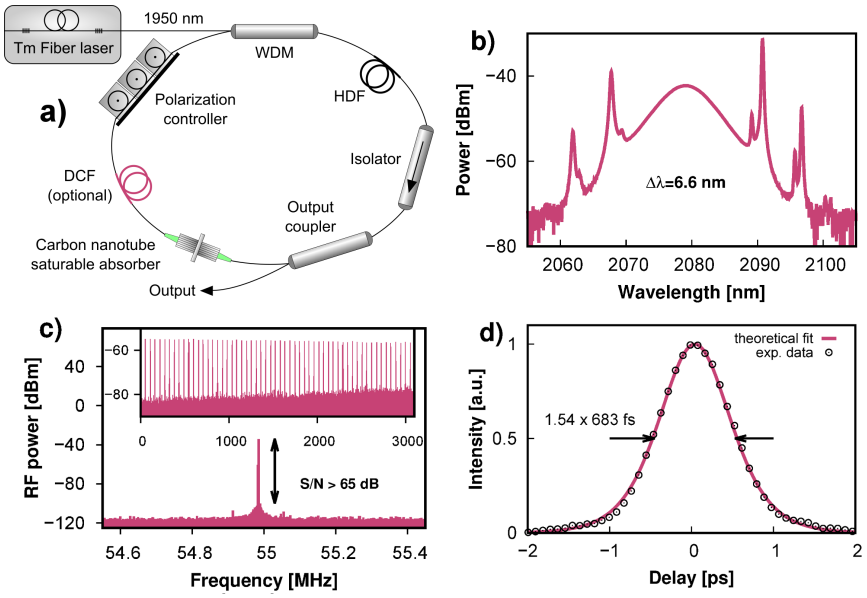

Fig. 4. Setup of the ring laser cavity (a). Performance of the laser operating in the solitonic regime with 400 nm thick CNT-SA and output coupling ratio of 30%: optical spectrum (b), radio frequency spectrum (c), and pulse autocorrelation (d).

Table 1. Influence of the m-SWCNT film thickness on laser performance. CNT - film thickness, λ_c - central wavelength, FWHM - optical bandwidth, F_{rep} - pulse repetition frequency, τ - pulse duration, P_p - pumping power, P_{avg} - average output power, E - pulse energy, TBP - time-bandwidth product. Output coupling ratio was fixed at 30%.

CNT [nm]	λ_c [nm]	FWHM [nm]	F_{rep} [MHz]	τ [fs]	P_p [W]	P_{avg} [mW]	E [pJ]	TBP
100	2086.5	4.72	54.43	991	0.81	8.2	151	0.322
200	2083.8	4.84	54.47	957	0.91	9.4	173	0.320
300	2082.4	6.35	54.36	717	1.10	19.8	364	0.315
400	2079.0	6.65	54.52	683	1.12	20.5	376	0.315

To confirm operation stability of the laser, optical spectra were recorded every 15 minutes over the course of 70 hours. The laser with 30% output coupling ratio and a 400 nm thick CNT-SA operated without any failure over the whole experiment period. The heatmap presented in Fig. 5 shows very little fluctuations in central wavelength and the optical bandwidth of the emitted pulses. We consider the result to be very satisfying, especially in terms of a non-PM, non-thermally-stabilized laser.

The output coupling ratio (OC) was increased in order to determine the maximum output power supported by the 400 nm CNT-SA in the solitonic regime. With the OC of 70%, the operation of the laser was stable and no degradation of the absorber was observed. A maximum of 74 mW output power corresponding to 1.35 nJ of pulse energy (at 54.9 MHz of repetition frequency) was achieved for a 400 nm thick CNT-SA.

Optics EXPRESS

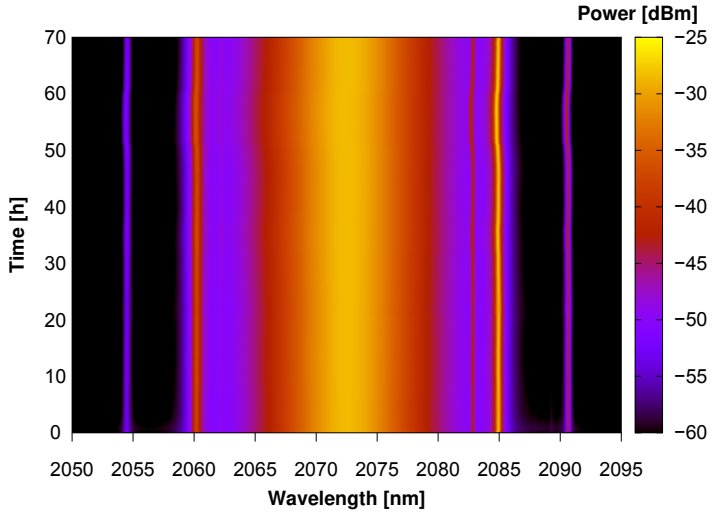

Fig. 5. Output optical laser spectra measured over the course of 70 hours.

4. Dispersion management

In order to determine whether the CNT-SAs support the operation in a stretched-pulse dispersion regime, a balanced-dispersion ring laser cavity was built by adding dispersion compensating fiber (DCF) to the all-anomalous dispersion laser. The dispersion tuning was realized by changing the length of the DCF while maintaining all other fibers and components of the laser cavity unchanged. The theoretical calculations conducted in order to choose appropriate fiber lengths were based on our dispersion measurements described previously [35]. In order to provide suitable modulation depth, a 700 nm thick CNT-SA was used. It was realized as a serial connection of a 300 nm and 400 nm thick CNT-SAs. The evolution of the output spectra affected by the net dispersion cavity is shown in Fig. 6(a) for a cavity with a 30% output coupling ratio. The broadest, 37 nm wide spectrum was generated by a laser with a net cavity dispersion of -0.007 ps^2. The average output power was in the range of 8-12 mW, and the repetition frequency varied between 20-28 MHz.

We have also performed output power scaling in a near-zero dispersion regime. At the highest OC value of 70% generated optical spectra was 31.4 nm wide (Fig. 6(b)), which corresponds to a theoretical, bandwidth-limited pulse duration of 198 fs. After canceling the pulses positive chirp by choosing the appropriate length of the output patchcord, 212 fs autocorrelation trace was recorded, as shown in Fig. 6(c). Further compression of the pulse duration would require higher-order dispersion compensation methods. The repetition frequency of the laser was 22.13 MHz, which is presented in Fig. 6(d) with a radio frequency spectrum. A very high average output power of 84 mW (pulse energy of 3.79 nJ) was reached. The obtained average output power is significantly higher than in a similar, graphene-based stretched-pulse laser [35], where only 54 mW of output power was generated for the same 70% output coupling ratio. The smaller optical bandwidth (than in the graphene-based setup) can be most likely explained by lower modulation depth of the CNT-SA.

Laser performance was characterized with the following equipment: optical spectrum analyzer (Yokogawa AQ6375), radio frequency spectrum analyzer (Keysight EXA N9010A) with a 16 GHz photodiode (Discovery Semiconductors DSC2-50S), Thorlabs PM100D power meter, and an autocorrelator (Femtochrome FR-103XL).

Optics EXPRESS

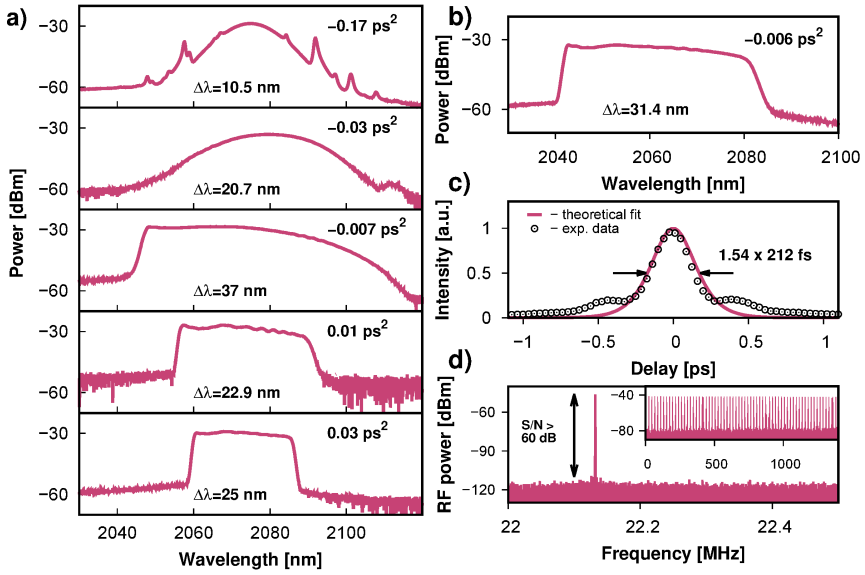

Fig. 6. Output optical spectrum evolution as a function of the net cavity dispersion (a). Optical spectrum (b), autocorrelation trace (c), repetition frequency and a radio frequency spectrum (d) of the laser with 70% output coupling ratio and -0.006 ps^2 of the net cavity dispersion measured at the highest average output power of 84 mW.

5. Conclusions

We have presented metallic CNT-SAs capable of stable and efficient operation in an ultrafast holmium-doped fiber laser. Thin films fabricated by vacuum filtration method were directly placed onto fiber connectors, forming fully fiberized saturable absorbers. In the solitonic regime, modifying the m-SWCNT film thickness in a CNT-SA can be used to tune central wavelength, pulse duration, and average output power in order to match the laser performance to desired parameters. The durability of the manufactured CNT-SAs was proven by providing stable mode-locking laser operation over the course of 70 hours. High average output powers (up to 74 mW) in soliton mode-locking are supported, which is a significant improvement over a similar, graphene-based laser [32]. By optimizing average output power in stretched-pulse dispersion regime 212 fs, 3.79 nJ pulses were generated directly from the oscillator.

To conclude, we believe that our results show that metallic carbon nanotube films can be used as a versatile and highly stable nanomaterial for nonlinear optical applications in the ~2080 nm wavelength range.

Funding

Polish Ministry of Science and Higher Education (IP2015 073774) and statutory funds of Chair of EM Field Theory, Electronic Circuits and Optoelectronics.

References

1. S. Y. Set, H. Yaguchi, Y. Tanaka, M. Jablonski, Y. Sakakibara, A. Rozhin, M. Tokumoto, H. Kataura, Y. Achiba, and K. Kikuchi, "Mode-locked fiber lasers based on a saturable absorber incorporating carbon nanotubes," in *OFC 2003 Optical Fiber Communications Conference,* (2003), p. PD44.
2. T. R. Schibli, K. Minoshima, H. Kataura, E. Itoga, N. Minami, S. Kazaoui, K. Miyashita, M. Tokumoto, and Y. Sakakibara, "Ultrashort pulse-generation by saturable absorber mirrors based on polymer-embedded carbon nanotubes," Opt. Express **13**, 8025–8031 (2005).

Optics EXPRESS

3. A. Schmidt, S. Rivier, G. Steinmeyer, J. H. Yim, W. B. Cho, S. Lee, F. Rotermund, M. C. Pujol, X. Mateos, M. Aguiló, F. Díaz, V. Petrov, and U. Griebner, "Passive mode locking of Yb:KLuW using a single-walled carbon nanotube saturable absorber," Opt. Lett. **33**, 729–731 (2008).
4. W. B. Cho, J. H. Yim, S. Y. Choi, S. Lee, A. Schmidt, G. Steinmeyer, U. Griebner, V. Petrov, D.-I. Yeom, K. Kim, and F. Rotermund, "Boosting the non linear optical response of carbon nanotube saturable absorbers for broadband mode-locking of bulk lasers," Adv. Funct. Mater. **20**, 1937–1943 (2010).
5. J. H. Im, S. Y. Choi, F. Rotermund, and D.-I. Yeom, "All-fiber Er-doped dissipative soliton laser based on evanescent field interaction with carbon nanotube saturable absorber," Opt. Express **18**, 22141–22146 (2010).
6. C. S. Goh, K. Kikuchi, S. Y. Set, D. Tanaka, T. Kotake, M. Jablonski, S. Yamashita, and T. Kobayashi, "Femtosecond mode-locking of a ytterbium-doped fiber laser using a carbon-nanotube-based mode-locker with ultra-wide absorption band," in *(CLEO). Conference on Lasers and Electro-Optics,* vol. 3 (2005), pp. 1644–1646.
7. E. J. Kelleher, J. C. Travers, Z. Sun, A. C. Ferrari, K. M. Golant, S. V. Popov, and J. R. Taylor, "Bismuth fiber integrated laser mode-locked by carbon nanotubes," Laser Phys. Lett. **7**, 790–794 (2010).
8. Y.-W. Song, S. Y. Set, S. Yamashita, C. S. Goh, and T. Kotake, "1300-nm pulsed fiber lasers mode-locked by purified carbon nanotubes," IEEE Photonics Technol. Lett. **17**, 1623–1625 (2005).
9. N. Nishizawa, Y. Seno, K. Sumimura, Y. Sakakibara, E. Itoga, H. Kataura, and K. Itoh, "All-polarization-maintaining Er-doped ultrashort-pulse fiber laser using carbon nanotube saturable absorber," Opt. Express **16**, 9429–9435 (2008).
10. K. Kieu and F. W. Wise, "Soliton thulium-doped fiber laser with carbon nanotube saturable absorber," IEEE Photonics Technol. Lett. **21**, 128–130 (2009).
11. A. Y. Chamorovskiy, A. V. Marakulin, A. S. Kurkov, and O. G. Okhotnikov, "Tunable Ho-doped soliton fiber laser mode-locked by carbon nanotube saturable absorber," Laser Phys. Lett. **9**, 602–606 (2012).
12. Y. Meng, Y. Li, Y. Xu, and F. Wang, "Carbon nanotube mode-locked thulium fiber laser with 200 nm tuning range," Sci. Reports **7**, 45109 (2017).
13. X. Liu, D. Han, Z. Sun, C. Zeng, H. Lu, D. Mao, Y. Cui, and F. Wang, "Versatile multi-wavelength ultrafast fiber laser mode-locked by carbon nanotubes," Sci. Reports **3**, 2718 (2013).
14. D. Li, H. Jussila, Y. Wang, G. Hu, T. Albrow-Owen, R. Howe, Z. Ren, J. Bai, T. Hasan, and Z. Sun, "Wavelength and pulse duration tunable ultrafast fiber laser mode-locked with carbon nanotubes," Sci. Reports **8**, 2738 (2018).
15. L. Hou, H. Guo, Y. Wang, J. Sun, Q. Lin, Y. Bai, and J. Bai, "Sub-200 femtosecond dispersion-managed soliton ytterbium-doped fiber laser based on carbon nanotubes saturable absorber," Opt. Express **26**, 9063–9070 (2018).
16. Z. Sun, T. Hasan, F. Wang, A. G. Rozhin, I. H. White, and A. C. Ferrari, "Ultrafast stretched-pulse fiber laser mode-locked by carbon nanotubes," Nano Res. **3**, 404–411 (2010).
17. L. N. Duan, L. Li, Y. G. Wang, and X. Wang, "All-fiber dissipative soliton laser based on single-walled carbon nanotube absorber in normal dispersion regime," Optik **137**, 308–312 (2017).
18. G. Sobon, A. Duzynska, M. Świniarski, J. Judek, J. Sotor, and M. Zdrojek, "CNT-based saturable absorbers with scalable modulation depth for Thulium-doped fiber lasers operating at 1.9 μm," Sci. Reports **7**, 45491 (2017).
19. X. Xu, S. Ruan, J. Zhai, L. Li, J. Pei, and Z. Tang, "Facile active control of a pulsed erbium-doped fiber laser using modulation depth tunable carbon nanotubes," Photon. Res. **6**, 996–1002 (2018).
20. Y.-W. Song, S. Yamashita, and S. Maruyama, "Single-walled carbon nanotubes for high-energy optical pulse formation," Appl. Phys. Lett. **92**, 021115 (2008).
21. S. Y. Set, H. Yaguchi, Y. Tanaka, and M. Jablonski, "Laser mode locking using a saturable absorber incorporating carbon nanotubes," J. Light. Technol. **22**, 51–56 (2004).
22. J. H. Yim, W. B. Cho, S. Lee, Y. H. Ahn, K. Kim, H. Lim, G. Steinmeyer, V. Petrov, U. Griebner, and F. Rotermund, "Fabrication and characterization of ultrafast carbon nanotube saturable absorbers for solid-state laser mode locking near 1 μm," Appl. Phys. Lett. **93**, 161106 (2008).
23. Z. Wu, Z. Chen, X. Du, J. M. Logan, J. Sippel, M. Nikolou, K. Kamaras, J. R. Reynolds, D. B. Tanner, A. F. Hebard, and A. G. Rinzler, "Transparent, conductive carbon nanotube films," Science **305**, 1273–1276 (2004).
24. S. Kobtsev, A. Ivanenko, Y. G. Gladush, B. Nyushkov, A. Kokhanovskiy, A. S. Anisimov, and A. G. Nasibulin, "Ultrafast all-fibre laser mode-locked by polymer-free carbon nanotube film," Opt. Express **24**, 28768–28773 (2016).
25. A. Chamorovskiy, A. Marakulin, S. Ranta, M. Tavast, J. Rautiainen, T. Leinonen, A. Kurkov, and O. Okhotnikov, "Femtosecond mode-locked holmium fiber laser pumped by semiconductor disk laser," Opt. Lett. **37**, 1448–1450 (2012).
26. K. Scholle, S. Lamrini, P. Koopmann, and P. Fuhrberg, "2 μm laser sources and their possible applications," in *Frontiers in Guided Wave Optics and Optoelectronics,* B. Pal, ed. (InTech, 2010).
27. S. Schilt, K. H. Tow, R. Matthey, M. Petersen, L. Thóvenaz, and T. Südmeyer, "First investigation of an all-fiber versatile laser frequency reference at 2 μm for CO2 lidar applications," in *International Conference on Space Optics — ICSO 2016,* vol. 10562 (International Society for Optics and Photonics, 2017), p. 105620I.
28. C. Kieleck, A. Hildenbrand, M. Eichhorn, D. Faye, E. Lallier, B. Gérard, and S. Jackson, "OP-GaAs OPO pumped by 2 μm Q-switched lasers: Tm; Ho: silica fiber laser and Ho: YAG laser," in *Technologies for Optical Countermeasures VII,* vol. 7836 (International Society for Optics and Photonics, 2010), p. 783607.
29. G. Liu, K. Yin, L. Yang, Z. Cai, B. Zhang, and J. Hou, "Noise-like pulse generation from a Ho-doped fiber laser based on nonlinear polarization rotation," in *2017 International Conference on Optical Instruments and Technology: Advanced Laser Technology and Applications,* vol. 10619 (International Society for Optics and Photonics, 2018), p. 1061908.

Optics EXPRESS

30. S. A. Filatova, V. A. Kamynin, N. R. Arutyunyan, A. S. Pozharov, A. I. Trikshev, I. V. Zhluktova, I. O. Zolotovskii, E. D. Obraztsova, and V. B. Tsvetkov, "Hybrid mode locking of an all-fiber holmium laser," JOSA B **35**, 3122–3125 (2018).
31. P. Li, A. Ruehl, C. Bransley, and I. Hartl, "Low noise, tunable Ho:fiber soliton oscillator for Ho:YLF amplifier seeding," Laser Phys. Lett. **13**, 065104 (2016).
32. J. Sotor, M. Pawliszewska, G. Soboń, P. Kaczmarek, A. Przewłoka, I. Pasternak, J. Cajzl, P. Peterka, P. Honzatko, I. Kasik, W. Strupinski, and K. Abramski, "All-fiber Ho-doped mode-locked oscillator based on a graphene saturable absorber," Opt. Lett. **41**, 2592–2595 (2016).
33. M. Pawliszewska, Y. Ge, Z. Li, H. Zhang, and J. Sotor, "Fundamental and harmonic mode-locking at 2.1 μm with black phosphorus saturable absorber," Opt. Express **25**, 16916–16921 (2017).
34. M. Hinkelmann, D. Wandt, U. Morgner, J. Neumann, and D. Kracht, "Mode-locked Ho-doped laser with subsequent diode-pumped amplifier in an all-fiber design operating at 2052 nm," Opt. Express **25**, 20522–20529 (2017).
35. M. Pawliszewska, T. Martynkien, A. Przewłoka, and J. Sotor, "Dispersion-managed Ho-doped fiber laser mode-locked with graphene saturable absorber," Opt. Lett. **43**, 38–41 (2018).
36. S. Y. Set, H. Yaguchi, Y. Tanaka, and M. Jablonski, "Ultrafast fiber pulsed lasers incorporating carbon nanotubes," IEEE J. Sel. Top. Quantum Electron. **10**, 137–146 (2004).
37. S. Xu, F. Wang, C. Zhu, Y. Meng, Y. Liu, W. Liu, J. Tang, K. Liu, G. Hu, R. C. Howe, T. Hasan, R. Zhang, Y. Shi, and Y. Xu, "Ultrafast nonlinear photoresponse of single-wall carbon nanotubes: a broadband degenerate investigation," Nanoscale **8**, 9304–9309 (2016).
38. H. Kataura, Y. Kumazawa, Y. Maniwa, I. Umezu, S. Suzuki, Y. Ohtsuka, and Y. Achiba, "Optical properties of single-wall carbon nanotubes," Synth. Met. **103**, 2555–2558 (1999).
39. M. Ouyang, J.-L. Huang, C. L. Cheung, and C. M. Lieber, "Energy gaps in "metallic" single-walled carbon nanotubes," Science **292**, 702–705 (2001).
40. Y. Matsuda, J. Tahir-Kheli, and W. A. Goddard, "Definitive band gaps for single-wall carbon nanotubes," The J. Phys. Chem. Lett. **1**, 2946–2950 (2010).
41. C. D. Spataru, S. Ismail-Beigi, L. X. Benedict, and S. G. Louie, "Excitonic effects and optical spectra of single-walled carbon nanotubes," Phys. Rev. Lett. **92**, 077402 (2004).
42. L. Lüer, G. Lanzani, J. Crochet, T. Hertel, J. Holt, and Z. V. Vardeny, "Ultrafast dynamics in metallic and semiconducting carbon nanotubes," Phys. Rev. B **80**, 205411 (2009).
43. A. Duzynska, M. Swiniarski, A. Wroblewska, A. Lapinska, K. Zeranska, J. Judek, and M. Zdrojek, "Phonon properties in different types of single-walled carbon nanotube thin films probed by Raman spectroscopy," Carbon **105**, 377–386 (2016).
44. G. Soboń, "Mode-locking of fiber lasers using novel two-dimensional nanomaterials: graphene and topological insulators [Invited]," Photonics Res. **3**, A56–A63 (2015).
45. T. Schibli, E. Thoen, F. Kärtner, and E. Ippen, "Suppression of Q-switched mode locking and break-up into multiple pulses by inverse saturable absorption," Appl. Phys. B **70**, S41–S49 (2000).